ASTFE
American Society
of Thermal and Fluids Engineers

5th-6th Thermal and Fluids Engineering Conference (TFEC)
May 26–28, 2021
Virtual Conference

TFEC-2021-36526

WAVELET TRANSFORMATION ANALYSIS APPLIED TO INCOMPRESSIBLE FLOW FIELD ABOUT A SOLID CYLINDER.

S. Sadeqi[1*], N. Xiros[1], S. Rouhi[1], J. Ioup[1], J. VanZwieten[2], C. Sultan[3],

[1]The University of New Orleans, 2000 Lakeshore Dr, New Orleans, LA 70148, USA.
[2]Florida Atlantic University, 777 Glades Road, EE316 Boca Raton, FL 33431, USA.
[3]Virginia Tech, 215 Randolph Hall, Blacksburg VA 24061, USA.

ABSTRACT

Flows past a circular cylinder develop in a variety of practical situations in engineering and in nature. One can properly focus on the study of beneficial cases and specifically attempt to harness this renewable clean energy resource to generate electrical power to help decrease air pollution and global warming. In addition, we need studies on stress and deformation of a circular cylinder due to the passing flow vortex in order to reduce the destructive effects, for example, on offshore structures. In this paper, we implement a two-dimensional numerical simulation with no-slip walls to monitor in detail how vortices are formed around a stationary circular cylinder when a shear current flows past a bluff body, namely a fixed circular cylinder. The Computational Fluid Dynamics (CFD) part of COMSOL Multiphysics was used to implement the continuity and Navier-Stokes equations that are based on the velocity field, pressure, and other preliminary variables. In the research reported here, various mathematical techniques such as various selected wavelet transforms over the space domain are applied to the exported data. A comprehensive wavelet numerical investigation is carried out on the vorticity and pressure field by using MATLAB software. Various Daubechies wavelets, Haar, Morlet, Paul and the m-th order derivative of Gaussian wavelets were tested to find the best wavelet transform to accurately analyze flow past a fixed cylinder. Numerical simulation results are compared with experimental data from the literature. An extensive comparative analysis is performed and discussed in detail in order to suggest improvements and expansions for the developed model.

KEY WORDS: Circular Cylinder, CFD, COMSOL, Wavelet Analysis, Haar, Daubechies, Paul, DOG, Morlet, MATLAB, Flow-Induced Vibration, Vorticity, Pressure Field.

1. INTRODUCTION

We encounter many problems, such as fatigue of offshore structures or the destructive effects of wind on skyscrapers, due to the static and dynamic loads on structures caused by fluid flow. Conducting experiments on flow-induced vibrations that correspond to the real physical situation is very expensive and time-consuming. However, computational solutions such as developing CFD [8] methods are able to simulate this challenging and destructive phenomenon.

*Corresponding Author: ssadeqi@uno.edu

A wavelet transform (WT) is the decomposition of a signal using a set of basis functions consisting of contractions, expansions, and translations of a function ψ(t), called the mother wavelet (Daubechies, 1991).[1] Many researchers have used wavelet transforms to analyze different characteristics of the fluid in laminar and turbulent flows. Orthonormal wavelet transforms are used to decompose velocity signals of turbulence into both space and scale.[2] A wavelet multi-resolution technique based on an orthogonal wavelet transform has been applied to analyzing the velocity data obtained simultaneously in two orthogonal planes in the turbulent near-wake of a circular cylinder. Using this technique, the flow is decomposed into a number of wavelet components based on their characteristic or central frequencies.[3] In these studies, research emphasized the turbulent regime for high Reynolds numbers. In this research, we attempt to use different wavelet transforms to find out what wavelets are appropriate to better reconstruct the pressure field, velocity and vorticity in both 1 and 2 dimensions. COMSOL Multiphysics single-phase flow (SPF) is used to simulate flow past a 2D stationary circular cylinder in a laminar, incompressible, Newtonian flow. The corresponding Reynold's number is 700 and Strouhal's number is very small (approximately 0.19).

2. THEORY[4]

2.1 Continuity and Navier-Stokes Equations

The governing equations to analyze the flow around a circular cylinder for an incompressible flow are the Continuity and Navier-Stokes equations. These equations are partial differential equations that characterize the motion of the fluids by considering boundary conditions such as inlet velocity, condition of the walls, and outlet pressure. In this paper, these equations will be solved numerically.

Equation (1) gives the most general differential form of the Continuity equation which describes the law of conservation of mass

$$\frac{\partial \rho}{\partial t} + \nabla.(\rho u) = 0 \qquad (1)$$

where ρ is the density (kg/ m^3), u is the velocity vector (m/s) and t is the time (s).

Constant density is a direct result of incompressible flow where the medium is sea-water, so equation (1) becomes equation (2), a scalar equation.

$$\nabla.u = o \qquad (2)$$

The Navier Stokes equation, Newton's second law for fluids is given in Equation (3). It is also known as the Transport equation, and shows the transport of linear momentum throughout the computational domain.[5]

$$(u.\nabla)u = -\frac{1}{\rho}\nabla P + \nu\nabla^2 u \qquad (3)$$

Where u is the velocity vector (m/s) and P is the pressure (Pa). The kinematic viscosity ν (m^2/s) can be viewed as viscous diffusivity or diffusivity for momentum[10] and defined as:

$$\nu = \frac{\mu}{\rho} \qquad (4)$$

where μ is the dynamic viscosity (Pa.s). A Petrov-Galerkin FEM method is used to discretize and solve equation (3) numerically.

2.2 Reynolds and Strouhal Number Analysis

The dimensionless Reynolds number describes a flow regime depending mainly on the ratio of the inertial forces and viscous forces in the fluid.[6]
Assuming the circular cylinder in this research

$$\mathrm{Re} = \frac{\text{Inertial Forces}}{\text{Viscous Forces}} = \frac{V_{ave}\, D}{\nu} = \frac{\rho V_{ave}\, D}{\mu} \qquad (5)$$

where V_{ave} is the average flow velocity (m/s) and D is the diameter of the circular cylinder (m).
Under most practical conditions, the flow in a circular pipeline is laminar at $\mathrm{Re} \leq 2300$; at $2300 \leq \mathrm{Re} \leq 4000$, transitional flow is observed; ultimately, at $4000 \leq \mathrm{Re}$, the flow becomes turbulent [6]. In monitored laboratory experiments, the laminar flow has been maintained at Reynolds numbers up to 100000. [6]. According to the geometry of the model (diameter D, initial velocity 1.4 m/s) considering the properties of sea-water, the Reynolds number for the current situation is about 700, in the laminar regime.
The vortex shedding frequency for most bluff body cylinders is given by[7]

$$f_s = \frac{St\, V}{D} \qquad (6)$$

where f_s is the vortex shedding frequency ($(\frac{1}{s})$, Hertz). [7].
The dimensionless Strouhal number (St) represents a measure of the ratio of inertial forces due to the unsteadiness of flow to the inertial forces due to changes in velocity.[5] It depends on the roughness or smoothness of the surface, as described by Achenbach and Heinecke (1981).[9] Many experiments have shown that there is a complicated relationship between the Strouhal number and Reynolds number.
In reference[10], the relationship between Reynolds and Strouhal numbers was demonstrated by Roshko[16,17], Kovasznay[18] and Tritton[19] for $\mathrm{Re} < 2 \times 10^4$ [10]. These have been used in the current model to specify the Strouhal number based on the given Reynolds number. According to reference[10], for the given Reynolds number (700), the corresponding Strouhal number is between approximately 0.19 and 0.2.
An empirical formula has been introduced for estimation of the Strouhal number by using the corresponding Reynolds number.[11]

$$St = 0.198\left(1 - \frac{19.7}{Re}\right) \qquad (7)$$

Substituting our computed Reynolds number into equation (7) gives the Strouhal number as 0.19. St numbers from the[10] and from the empirical formula show reasonable agreement.

2.3 Wavelet Transform Theory [12]

Wavelet transforms are a useful and practical tool in many areas. A wavelet is a mathematical function used to divide a given function or continuous-time signal into different scale components. Usually, one can assign a frequency range to each scale component. Each scale component can then be studied with a resolution that matches its scale. A wavelet transform is the representation of a function by wavelets.[13] The wavelets are scaled and translated versions of a finite-length or fast-decaying oscillating waveform (the mother wavelet). Wavelet transforms have advantages over traditional Fourier Transforms for representing functions that have discontinuities and sharp peaks, and for accurately deconstructing and reconstructing finite, non-periodic signals.[13]
By using convolution with the wavelets and a disturbed signal, we are able to construct an unknown section of the signal. The forward Wavelet transform of a function $f(t)$ with respect to wavelet $w(t)$ is

$$F_w(s,a) = \frac{1}{\sqrt{a}}\int_{-\infty}^{+\infty} f(t)w\left(\frac{t-s}{a}\right)dt. \qquad (8)$$

$$w_{a,s}(t) = \frac{1}{\sqrt{a}}w\left(\frac{t-s}{a}\right) \qquad (9)$$

Where $a \neq o$ is the scale parameter and s is the translation parameter.

i. Haar Wavelet[12]

A wavelet is a small wave. In Haar's case it is a square wave.[12] The Haar wavelet H(t) is defined to be the difference of two half-boxes:

$$H(t) = \varphi(2t) - \varphi(2t-1) = \begin{cases} 1 & 0 \le t \le \frac{1}{2} \\ -1 & \frac{1}{2} \le t \le 1 \end{cases} \qquad (10)$$

Where $\varphi(t)$ represents a box function and its dilation $\varphi(2t-1)$ represents a half-box function.[12]

ii. Daubechies Wavelet

The Daubechies wavelets were invented by researcher Ingrid Daubechies as a family of orthogonal wavelets. If W is a wavelet with p vanishing moment that generates orthonormal basis of $L^2(\mathbb{R})$, then it has a support of size larger than or equal to 2p-1. A Daubechies wavelet has a minimum size support equal to [-p+1, p].[14]

The mathematical equation of the Daubechies filter D(t) is:

$$D(t) = \left(\frac{1+\cos t}{2}\right)^2 \sum_{k=0}^{p-1} \binom{p-1+k}{2} \left(\frac{1-\cos t}{2}\right)^k \qquad (11)$$

iii. Morlet Wavelet[15]

The complex Morlet wavelet (Gabor wavelet) is a sine function tapered by a complex Gaussian window. The width of the Gaussian window has a direct effect on the accuracy of the Morlet wavelet transform. The mathematical form of a complex Morlet wavelet W(t) is:

$$W(t) = e^{2\pi i f t} e^{-\frac{t^2}{2\sigma^2}} \qquad (12)$$

where $\boldsymbol{i}$ indicates the imaginary unit, f (Hz) is the frequency, σ is the width of the Gaussian window and t (s) shows the time.

iv. Paul Wavelet [16]

The Paul wavelet contains few oscillations but is very localized in time. This will give a very accurate time resolution but a reduced frequency resolution.[17]

The orders of the Paul wavelets start from 4, and the default smallest scale is 2 Δt, where Δt is the sampling period [16]. The mathematical form of the Paul wavelet $\psi(t)$ is:[17]

$$\psi(t) = \frac{2^k i^k k!}{\sqrt{\pi(2\pi)!}}(1-it)^{-(k+1)} \qquad (13)$$

The value of k controls the number of oscillations present in the mother wavelet and, hence, will strongly influence the frequency and time resolution of the corresponding wavelet transform.[17]

v. M-th Order Derivative of Gaussian Wavelet: (DOG)[16]

The $\chi(t)$ DOG wavelet has relatively few oscillations in a much wider time domain. Note that both the Morlet and the Paul wavelet are complex-valued, whereas the Derivative of Gaussian wavelet is real-valued. [6]

$$\chi(t) = \frac{(-1)^{k+1}}{\sqrt{\Gamma\left(k+\frac{1}{2}\right)}} \frac{d^k}{dt^k}\left(e^{-\frac{t^2}{2}}\right) \qquad (14)$$

where Γ indicates the Gamma function. The Derivative of Gaussian wavelet with k = 2 is also referred to as the 'Mexican hat' wavelet.[17]

3. Numerical Method

Figure 1 shows a two-dimensional (2D) scheme of the computational domain for flow past a circular cylinder. The diameter of the circular cylinder is D. Based on the diameter of the cylinder, the height and width of the rectangular computational domain are defined as 10D and 32D. As shown in figure 1, the inlet flow is from the left-hand side of the computational domain. The velocity of the inlet flow is defined to be linear at 1.4 m/s.

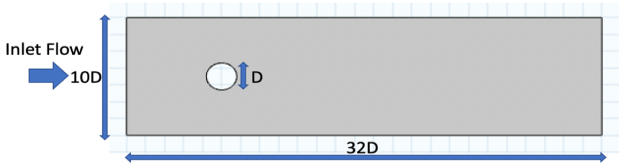

Figure 1. Scheme of the 2D computational domain

Figure 2 gives the computational mesh close to the circular cylinder. Finding the most accurate mesh is a very crucial and time-consuming step in the simulation process since it is directly related to the accuracy of the results. In this computational mesh, the maximum element size is 0.0315D and the minimum element size is 0.0014D. For corner refinement and free triangular sections, the curvature factor is specified to be 0.3. For sharp corners, trimming is used, in which the minimum angle for trimming is 240 degrees and the maximum angle for trimming is 50 degrees. In addition, the maximum layer decrements are 2. Ultimately, for a smooth transition to the interior mesh, the number of iterations was determined to be 8 and the maximum element depth to process to be 16 elements.

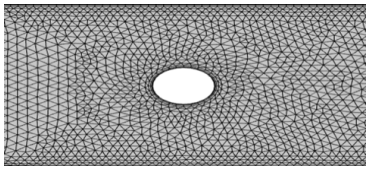

Figure 2. Scheme of the 2D computational mesh around the circular cylinder

4. Computational Results

The wavelet analyzer of MATLAB was used for wavelet transforms. There are some articles using wavelet transforms in different aspects of fluid mechanics. Wang, So and Xie presented wavelet analysis of flow-induced forces on two stationary cylinders by considering the Reynolds number effect ($60 \leq \mathrm{Re} \leq 200$). Their results were compared with experimental measurements and theoretical predictions and show good agreement.[18] Zhao, Cheng and An carried out a numerical investigation of Vortex-Induced vibration of a circular cylinder in the transverse direction in oscillatory flow by using the continuous Morlet wavelet transform in the turbulent regime for different KC numbers.[19]

4.1 Wavelet transform analysis for 2D pressure field, velocity field, and vorticity

In figures 3, 4 and 5, the top row shows the surface and contour plots of the pressure field, velocity field and vorticity once the circulation motion is formed close to the bluff body (cylinder). The other rows present different wavelet transforms that show reasonable reconstruction in comparison to other wavelet transforms. The last rows show the specific wavelet that gives the best reconstruction. To analyze the pressure field, velocity field, and vorticity, Morlet wavelets of order (1, 2, …, 10), Paul wavelets of order (4, 5, …, 10) and DOG wavelets of order (2,4, …, 10) were used. For each specific wavelet, the wavelets that best reconstructed the signals were chosen and given in the figures below. The red solid lines show the original signals and the blue solid lines indicate the wavelet reconstructed signals in each figure. Specifically, in figure 3, different wavelet transforms in different orders were examined for the pressure field. Among different orders of the Paul wavelet, Paul 4 reconstructs the original signal better than the others. In the case of the Morlet wavelet, the reconstruction of the Morlet 5 shows a closer result to the original signal than other orders of this wavelet. Finally, DOG 8 illustrates better reconstruction than other orders. The Morlet 5, Paul 4, and DOG 8 are the best wavelets to reconstruct the original pressure field signal. Between these three wavelets, it is clear that DOG 8 is the best wavelet for this specific signal. It perfectly reproduced the signal upstream and downstream. In figure 4, the results of the various wavelet transforms for the velocity field were shown. The Paul 8 shows better results compare to other orders of the Paul wavelet. In the case of the DOG wavelet, DOG 8 indicates better reconstruction than other DOG wavelets.

Wavelet analysis of the vorticity is shown in figure 5. The Morlet 5 shows better reconstruction than DOG 8 and Paul 8, especially in the wake. The best wavelet transform reconstruction of the vorticity signal is the Paul 10 wavelet.

Table 1 provides a summary of the wavelets tested and results with respect to the 2D signals of the pressure field, velocity and vorticity.

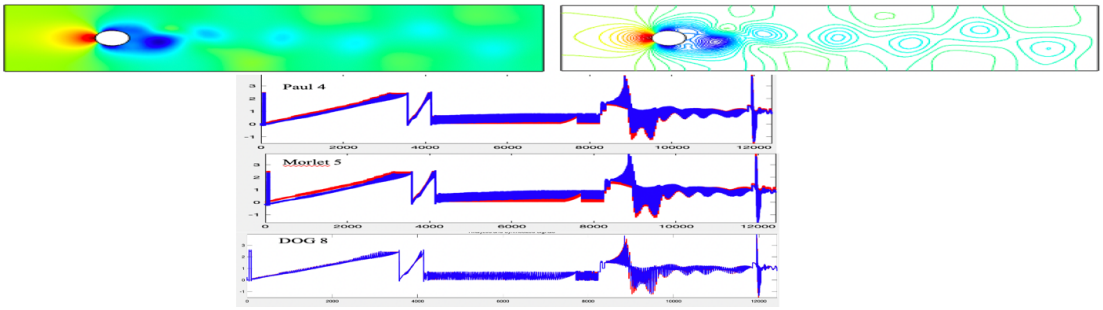

Figure 3. 2D wavelet analysis of the pressure field

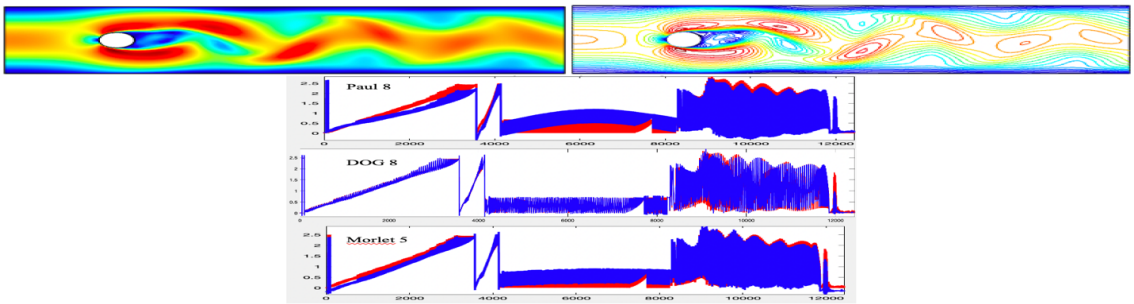

Figure 4. 2D wavelet analysis of the velocity field

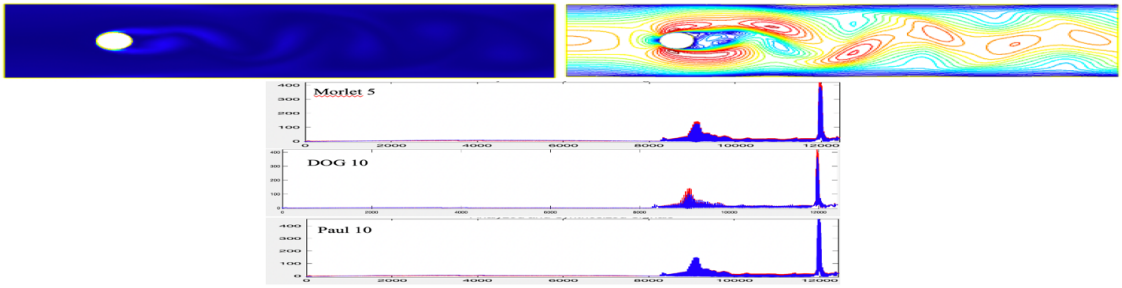

Figure 5. 2D wavelet analysis of the vorticity

Order of the Wavelet	Morlet Wavelet	Paul Wavelet	DOG Wavelet	Perfect Reconstruction
1	Done	-	-	
2	Done	-	Done	
3	Done	-	-	
4	Done	Done. Best in the case of the Pressure	Done	
5	Done. Best in the case of the Pressure, Velocity and Vorticity	Done	-	Morlet 5 Shows Perfect Reconstruction for the Velocity Field.
6	Done	Done	Done	
7	Done	Done	-	
8	Done	Done. Best in the case of the Velocity	Done. Best in the case of the Pressure and Velocity.	DOG 8 Shows Perfect Reconstruction for the Pressure Field.
9	Done	Done	-	
10	Done	Done. Best in the case of the Vorticity	Done. Best in the case of the Vorticity	Paul 10 Shows Perfect Reconstruction for the Vorticity.

Table 1. Summary of wavelet analysis of the pressure field, velocity and vorticity

4.2 Wavelet transform analysis for 1D pressure field, velocity field, and vorticity at the top of the circular cylinder

To analyze the 1-dimensional pressure, velocity and vorticity, a cutline at the top of the cylinder is defined as shown in figure 6. In addition to the Morlet, Paul, and DOG wavelets that were examined for 2D fluid properties, Haar and Daubechies wavelets (various orders) were also tested.

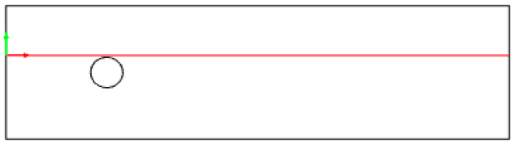

Figure 6. Schematic of a cutline (1D) on top of the circular cylinder

For figures 7, 8, and 9, as before, the red solid lines show the original signals and the blue indicates the reconstruction for specific wavelet transforms. In figure 7, different wavelet transforms were applied to the original pressure field signal after the circulation pattern was created around the cylinder. The result of the Hear wavelet is acceptable; for different orders of the Daubechies wavelet, db5 looks better than others. Morlet 3 shows better signal reconstruction than other orders. Although none of the orders of the Paul wavelet indicates reasonable reconstruction for this specific signal, Paul 7 was the best. From different orders of the DOG wavelet, DOG 8 was chosen as the best reconstruction of the 1D pressure signal.
Results show in figure 8 that the behavior of the Haar, Morlet 3, DOG 8, and Daubechies wavelets are acceptable again, but, similar to the pressure, the Paul wavelet did not reconstruct the 1D velocity signal very well. In this case, Db5 was chosen as the best reconstruction wavelet for the velocity signal.
Figure 9 shows that the Haar, Db5, and DOG 8 give good reconstruction for the vorticity signal. Unlike, the pressure and velocity, Here the different orders of the Paul wavelet show good results for analyzing the vorticity, especially Paul 5. The Morlet 6 was chosen as the best reconstruction wavelet for the vorticity signal, especially in the regions of the spikes.
Table 2 gives a summary of the analyzing wavelets and their effects on the pressure field, velocity, and vorticity signals in 1D.

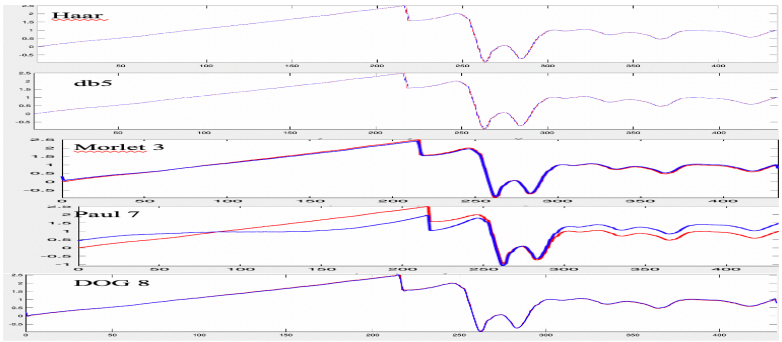

Figure 7. 1D wavelet analysis of the pressure field at the cutline on top of the circular cylinder

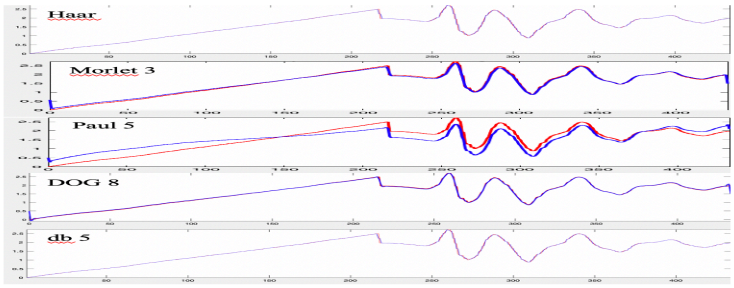

Figure 8. 1D wavelet analysis of the velocity field at the cutline on top of the circular cylinder

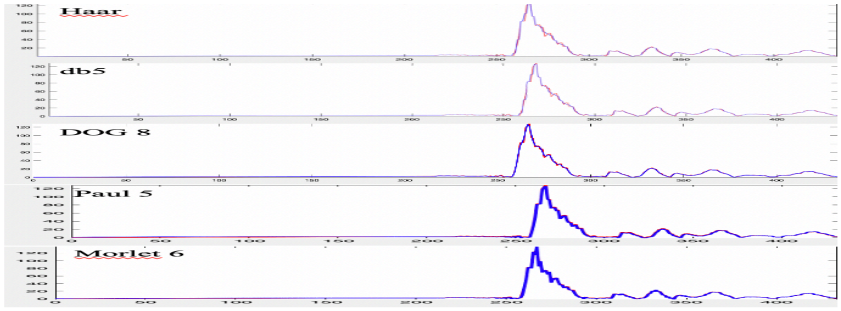

Figure 9. 1D wavelet analysis of the vorticity field at the cutline on top of the circular cylinder

Order of the Wavelet	Haar Wavelet	Daubechies Wavelet	Morlet Wavelet	Paul Wavelet	DOG Wavelet	Perfect Reconstruction
1	Done	Done	Done	-	-	
2	-	Done	Done	-	Done	
3	-	Done	Done. Best in the case of the Pressure and Velocity	-	-	
4	-	Done	Done	Done	Done	
5	-	Done. Best in the case of the Pressure, Velocity and Vorticity	Done	Done. Best in the case of the Velocity and Vorticity	-	Daubechies 5 Shows Perfect Reconstruction for the Velocity Field.
6	-	Done	Done. Best in the case of the Vorticity	Done	Done	Morlet 6 Shows Perfect Reconstruction for the Vorticity.
7	-	Done	Done	Done. Best in the case of the Pressure	-	
8	-	Done	Done	Done	Done. Best in the case of the Pressure, Velocity and Vorticity	DOG 8 Shows Perfect Reconstruction for the Pressure Field.
9	-	Done	Done	Done	-	
10	-	Done	Done	Done	Done	

Table 2. Summary of 1D wavelet analysis of the pressure field, velocity and vorticity

5. Conclusions

In general, the Haar, Db5, DOG 8, and Morlet 3 are the best candidate wavelets for 1D analysis of fluid properties. The results using the Paul wavelet for the pressure and velocity fields were not good. It needs future study; one of the difficulties could be different close peaks and asymmetric oscillations as this wavelet is not able to reconstruct this kind of signal.
In the case of 2D fluid analysis of the pressure, velocity, and vorticity, Morlet 5 and DOG 8 show acceptable results. These wavelets properly reconstruct various signals in different situations such

as upstream, downstream, and around the bluff body (cylinder). Their reconstructions in the peaks of the signals are very good.

ACKNOWLEDGMENT

The authors would like to thank the National Science Foundation (NSF) and specifically the Energy, Power, Control and Networks (EPCN) program for their valuable ongoing support in this research within the framework of grant ECCS-1809182 'Collaborative Research: Design and Control of Networked Offshore Hydrokinetic Power-Plants with Energy Storage'.

REFERENCES

[1] E.A.B. Da Silva, D.G. Sampson, in Advances in Imaging and Electron Physics, *Successive Approximation Wavelet. Vector Quantization for Image and Video Coding.* (1996). **Book**
[2] H. Moori, H. Kubotani, T. Fujitani, H. Niino and M. Takaoka, Wavelet analysis of velocities in laboratory isotropic turlence, Fluid Mech., 389 pp 229-248, (1999). **Journal Paper**
[3] R. Rinoshinka and Y. Zhou, Orthonormal Wavelet multi-resolution analysis of a turbulent cylinder wake, J. fluid Mech,.524, pp. 229-248, (2005), **Journal Paper**
[4] COMSOL CFD user guild (Version 5.4), **Book**
[5] Munson Young Okiishi, Fundamentals of Fluid Mechanics, Fifth Edition, John Wiley and Sons, Inc, page 365 and 854, **Book**
[6] https://en.wikipedia.org/wiki/Isotropic_solid, **Web Document**
[7] https://www.engineeringtoolbox.com/poissons-ratio- d 1224.html, **Web Document**
[8] S Rouhi, S Sadeqi, N Xiros, J Ioup, CFD analysis of Filling Process for a Hydrogen Energy Storage System, 5th Thermal and Fluids Engineering Conference (TFEC), (2020), **Conference Paper**
[9] Mohammad Hosny Eid, Vortex Shedding from Single and Tandem Finned cylinders, Thesis, McMaster University, (2004). **Thesis**
[10] ohn H. Lienhard, Synopsis of Lift, Drag, and Vortex Frequency Data for Rigid Circular Cylinder, Washington State University, College of Engineering, (1966), **Web Document**
[11] http://www.thermopedia.com/content/1247/ Bengt Sunden, Vortex Shedding, Online resource. **Web Document**
[12] Gilbert Strang, Triung Nguyen, Wavelets and Filter Banks, Wellesley-Cambridge Pres, Wellesley, MA 02181, **Book**
[13] https://en.wikipedia.org/wiki/Wavelet, **Web Document**
[14] téphaneMallat , in A Wavelet Tour of Signal Processing (Third Edition), (2009), **Web Document**
[15] Michael X Cohen, A better way to define and describe Morlet wavelet for time-frequency analysis, Radboud University, **Web Document**
[16] Matlab Website; https://www.mathworks.com/help/wavelet/ref/cwtft.html, **Web Document**
[17] I. Demoortel, A.W. Hood, Wavelet Analysis: the effect of varying basic wavelet parameters, Article in Solar Physics · January 2004 DOI: 10.1023/B:SOLA.0000043578.01201.2d, **Journal Paper**
[18] X.Q. Wang, R.M.C. So and Wei-Chau Xie, Wavelet Analysis of Flow-Induced Forces on Two Side-by-Side Stationary Cylinders: Reynolds Number Effect, ASME 2006, Pressure Vessels and Piping Divisions, **Conference Paper**
[19] Ming Zhao, Liang Cheng and Hongwei An, Numerical investigation of Vortex-Induced vibration of a circular cylinder in transverse direction in oscillatory flow, Ocean Engineering, January (2012), **Journal Paper**
[20] J. Lee, S.I. Lee, C.W. Park, Reducing the drag on a circular cylinder by upstreaminstallation of a small control rod, Fluid Dynam. Res. 34 (2004) 233–250. **Journal Paper**
[21] M. Ozgoren, Flow structure in the downstream of square and circular cylinders, Flow Measure. Instrum. 17 (2006), **Journal Paper**
[22] X. Gilliam, J. Dunyak, A. Doggett, D. Smith, Coherent structure detection usingwavelet analysis in long time-series, J. Wind Eng. Ind. Aerodyn. 88 (2000) 83–195, **Journal Paper**
[23] Ma, G.-S. Karamanos, G. Karniadakis, Dynamics and low-dimensionalityof a turbulent near wake, J. Fluid Mech. 410 (2000) 29–65, http://dx.doi.org/10.1017/S0022112099007934. **Journal Paper**
[24] Cao, T. Tamura, H. Kawai, Spanwise resolution requirements for thesimulation of high-reynolds-number flows past a square cylinder, Comput.& Fluids 196 (2020) http://dx.doi.org/10.1016/j.compfluid.2019.104320. **Journal Paper**
[25] Cao, T. Tamura, Shear effects on flows past a square cylinder withrounded corners atRe=2.2×104, J. Wind Eng. Ind. Aerodyn. 174 (2018)119–132, http://dx.doi.org/10.1016/j.jweia.2017.12.025. **Journal Paper**
[26] De Stefano, G., & Vasilyev, O. Wavelet adaptive simulation of three-dimensional flow past a square cylinder. Journal of Fluid Mechanics, 748, 433-456. Doi:10. 1017/jfm.2014.193, (2014). **Journal Paper**
[27] Brun, C., Aubrun, S., Goossens, T. & Ravier, Ph. Coherent structures and their frequency signature in the separated shear layer on the sides of a square cylinder. Flow Turbul. Combust. 81, 97–114. (2008). **Journal Paper**

[28] Yiu M. W., Zhou Y., Zhou T. and Cheng L.,"Reynolds number effects on 3-D vorticity in a turbulent wake", AIAA Journal, Vol.42, pp.1009-1015, (2004). **Journal Paper**

[29] K. Schneider, M. Farge, F. Koster, and M. Griebel, "Adaptive Wavelet Methods for the Navier–Stokes Equations," Notes on Numerical Fluid Mechanics (E. H. Hirschel, Ed.), pp. 303–318, Springer-Verlag, Berlin/New York, (2001). **Book**

[30] K. Schneider and M. Farge, Computing and analysing turbulent flows using wavelets, in "Wavelet Transforms and Time-Frequency Signal Analysis" (L. Debnath, Ed.), pp. 181–216, Birkhäuser, Boston, (2001), **Journal Paper**